Bistability and non-monotonic induction of the *lac* operon in the natural lactose uptake system

D. Zander, D. Samaga, R. Straube, K. Bettenbrock

Abstract

The *E. coli lac* operon is regulated by a positive feedback loop whose potential to generate an all-or-none response in single cells has been a paradigm for bistable gene expression. However, so far bistable *lac* induction has only been observed using gratuitous inducers raising the question about the biological relevance of bistable *lac* induction in the natural setting with lactose as the inducer. In fact, the existing experimental evidence points to a graded rather than an all-or-none response in the natural lactose uptake system. In contrast, predictions based on computational models of the lactose uptake pathway remain controversial. While some argue in favor of bistability others argue against it. Here, we reinvestigate *lac* operon expression in single cells using a combined experimental / modeling approach. To this end we parametrize a well-supported mathematical model using transient measurements of LacZ activity upon induction with different amounts of lactose. The resulting model predicts a monostable induction curve for the wildtype system, but indicates that overexpression of the LacI repressor would drive the system into the bistable regime. Both predictions were confirmed experimentally supporting the view that the wildtype *lac* induction circuit generates a graded response rather than bistability. More interestingly, we find that the *lac* induction curve exhibits a pronounced maximum at intermediate lactose concentrations. Supported by our data a model-based analysis suggests that the non-monotonic response results from saturation of the LacI repressor at low inducer concentrations and dilution of Lac enzymes due to an increased growth rate beyond the saturation point. We speculate that the observed maximum in the lac expression level helps to save cellular resources by limiting Lac enzyme expression at high inducer concentrations.

Introduction

The lactose utilization system of *E. coli* is encoded by the *lac* operon which consists of a regulatory promoter-operator region and three structural genes *lacZYA* (1). While the gene products of *lacY* and *lacZ* are involved in uptake and cleavage (metabolism) of lactose (*lacY* encodes lactose permease, *lacZ* encodes ß-galactosidase, Fig. 1) the function of the transacetylase LacA is less clear (2). Induction of the *lac* operon by lactose or by the well-studied gratuitous inducers IPTG and TMG is controlled by the lactose repressor LacI. In the absence of lactose *lac* gene expression is strongly repressed by LacI through formation of a DNA loop which preferably occurs between the main operator (O_1) and one of the auxiliary operators (O_2 and O_3) (3) (Fig. 1). If present, lactose is actively transported into the cell by lactose permease (1). Intracellular lactose is metabolized by LacZ in two distinct reactions: The disaccharide is either cleaved into the monosaccharides glucose and galactose which are used for cell growth or it is converted into its isomer allolactose which represents the natural inducer of the *lac* operon (2). Through sequestration of the LacI repressor allolactose prevents binding of the repressor to the operator sites.

Since both enzymes, LacY and LacZ, are involved in the generation of the inducer of their own synthesis there exists a positive feedback loop in the *lac* regulatory system that may potentially lead to bistability (4). However, since lactose is also actively metabolized increased levels in the amount of LacY and LacZ do not only lead to the production of more inducer molecules, but also increase the growth rate which, in turn, leads to a faster dilution of the Lac enzymes as well as of the inducer. Theoretical studies have shown that this negative feedback may substantially weaken the positive feedback loop (5, 6) which has contributed to the prevailing opinion that bistability is unlikely to be observed in the natural lactose utilization system (5, 7, 8). Consistent with this argument bistable induction behavior has so far only been observed using artificial inducers, such as TMG (9, 10) or IPTG (11, 12), where *lac* gene induction is essentially decoupled from cell growth: While uptake of gratuitous inducers is still catalyzed by LacY they are not metabolized by LacZ. Instead, internalized TMG and IPTG induce *lac* gene expression through direct binding to the LacI repressor.

In addition to control by LacI, *lac* operon expression is also controlled by carbon catabolite repression (13). The transcriptional activator complex CRP-cAMP is necessary for efficient transcription of the *lac* operon, and it has been suggested to enhance DNA looping (14). Its concentration is kept low in the presence of glucose, the preferred substrate of *E. coli*. In addition, glucose becomes phosphorylated while entering the cell through a sequence of reactions mediated by the PEP-dependent phosphotransferase system (PTS). In the course of this process the glucose-specific PTS protein $EIIA^{Glc}$ becomes dephosphorylated which then binds to LacY and inhibits the uptake of lactose, a process termed inducer exclusion.

Even though several theoretical studies came to the conclusion that bistability would be unlikely to occur if lactose is the only galactosidic carbon source in the medium it remains controversial what to expect in the presence of lactose *and* glucose. While some authors argue in favor of bistability (5, 15, 16) others argue against it (6, 17). Interestingly, Savageau has derived a design principle (6) which summarizes, in a mechanism-independent manner, the conditions under which bistability may exist in the natural lactose utilization system. From his analysis, it follows that glucose-mediated effects such as catabolite repression and inducer exclusion make it more difficult to satisfy the conditions required to generate bistability. The design principle also indicates that the natural *lac* circuit is protected from bistability by the fact that the inducer is an intermediate of the inducible pathway, but that alternative fates of the intermediate, such as LacY-independent excretion from the cell, may promote bistability. Another prediction of the Savegeau design principle is that the likelihood of bistability can be increased by increasing the effective cooperativity with which the inducer affects the transcription rate of *lac* genes. Consistent with this prediction Narang and Pilyugin argue that DNA looping, which is known to increase the cooperativity of repressor-operator interactions, is essential to overcome the attenuating effect of growth rate-dependent dilution and to promote bistability (5). Together, these results suggest that if the natural lactose utilization system exhibits bistability, the probability to observe it experimentally is largest in the absence of glucose. Conversely, if bistability is not observed in the natural system increasing repressor-operator cooperativity through overexpression of LacI could be one means to drive the natural system into a regime where it may exhibit bistability.

To test these ideas we employed a combined experimental and computational modeling approach which indicates that the natural lactose system operates near, but not in the bistable regime. Through overexpression of LacI we could observe bimodal distributions of cells in a culture, which suggests that LacI overexpression, indeed, leads to bistable induction behavior – in agreement with previous theoretical predictions. Noticeably, in the absence of bistability the stimulus-response curve of LacZ induction exhibits a pronounced maximum at intermediate lactose concentrations which can be rationalized using our computational model.

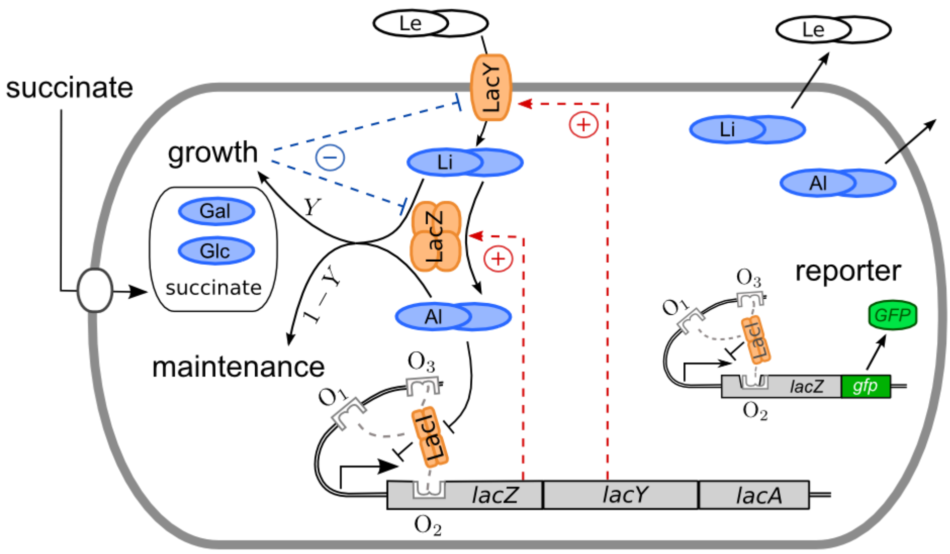

Fig. 1: Scheme of lactose metabolism, gene expression and model setup. Cells grown on succinate are induced with different amounts of lactose (Le). Internalized lactose (Li) is converted into allolactose (Al). Sequestering of LacI repressor by allolactose induces the synthesis of LacY and LacZ and creates a positive feedback loop (dotted lines). Both lactose and allolactose are also used for growth and maintenance so that an increased uptake rate also increases the dilution rate of the lac enzymes which weakens the positive feedback loop. Cells contain a GFP reporter under the control of a native *lac* promoter.

Methods

Choice of parameter values

Lactose import

To describe lactose uptake into the cell we consider LacY-mediated influx as well as lactose excretion due to leak fluxes. The LacY permease is a galactoside:H symporter which utilizes the proton motive force (pmf) to actively pump lactose and protons (1:1 stoichiometry) into the cell (18). We model the import of lactose by a saturable function of the form (5)

$$V_L[LacY]\frac{[Le]}{K_L+[Le]} \qquad \text{(M1)}$$

where V_L and K_L denote the turnover number of LacY and the half-saturation constant, respectively. The former has been measured in EDTA-treated cells as $\bar{V}_L = 48/s$ [Wright et al., 1981] or, rewritten in relative mass units (cf. Table S1),

$$V_L = \bar{V}_L\frac{mp_L}{mp_Y} = 1271\frac{\frac{g_L}{gdw}}{\frac{g_Y}{gdw}}\frac{1}{h}.$$

The value of the half-saturation constant has been reported to depend on the pmf. In membrane vesicles its value ($\overline{K_L}$) lies between $85\mu M$ and $200\mu M$ (19, 20). However, as the pmf decreases the value of the half-saturation constant increases up to $14mM$ (20). Because the value determined for vesicles might not be appropriate to describe the situation in cells we left K_L as a free parameter to be determined by fitting the model to experiments. In that way we obtained $K_L = 0.68\ g/l$ or $\overline{K_L} \approx 2mM$ which lies halfway between 0.2mM and 14mM. To convert the unit of $\overline{K_L}$ into g/l (as required for Eq. 1) we have used the relation

$$K_L = \overline{K}_L \cdot 10^{-6} \cdot m_L$$

where $\overline{K}_L$ is measured in μM and m_L denotes the molar mass of lactose (cf. Table S1).

Efflux of lactose and allolactose

Measurements of the lactose uptake rate suggest that part of the internalized lactose is again excreted by the cell due to the presence of leak fluxes (18). For the non-metabolisable inducer TMG an excretion rate of $k_e^- = 60/h$ has been reported (21). Another study showed that more than half of the products of the LacZ-catalyzed reaction (i.e. glucose, galactose and allolactose) can be observed in the medium in less than 60 min after addition of lactose (22) suggesting that the excretion rates of allolactose and TMG are comparable (although the mechanism by which allolactose leaves the cell is unknown). Due to the structural similarity between lactose and allolactose we use the same value for the excretion rate constant ($k_e^- = 60/h$) for both substrates.

Inducer exclusion

The glucose, which is produced as part of the LacZ-mediated metabolization of lactose and allolactose, negatively regulates Lac enzyme expression by two mechanisms: (i) catabolite repression (by inactivation of cAMP synthase) and (ii) inducer exclusion (through dephosphorylation of the PTS enzyme IIA^{GLC}). According to previous studies inducer exclusion appears to be the more dominant mechanism by which *lac* gene expression is downregulated (23, 24). Therefore, we decided to include this mechanism, albeit in a simplified manner. To this end, we first note that intracellularly produced glucose becomes phosphorylated by IIA^{GLC} in a phosphotransfer reaction, in the course of which IIA^{GLC} is dephosphorylated. Unphosphorylated IIA^{GLC} then binds to LacY acting as an uncompetitive inhibitor (25, 26) which suggests modifying the expression for the import rate in Eq. (M1) as

$$V_L[LacY]\frac{[Le]}{K_L + [Le]\left(1 + \frac{[IIA^{GLC}]}{K_{II}}\right)} \tag{M2}$$

To relate the concentration of IIA^{GLC} to quantities in our model we assume, for simplicity, a linear relation between glucose levels and $[IIA^{GLC}]$ and, similarly, for the relation between glucose and intracellular lactose. The latter assumption is justified by the fact that in simulations the intracellular lactose concentration never exceeded the Km value for LacZ. Under these assumptions we may rewrite Eq. (M2) in the form

$$V_L[LacY]\frac{[Le]}{K_L + [Le]\left(1 + \frac{[Li]}{K_i}\right)} \tag{M3}$$

which describes the inhibition of the LacY-mediated import of lactose in an effective manner. In Eq. (M3) the parameter K_i denotes an apparent inhibition constant to be determined by fitting the model to experiments.

Repressor-inducer interaction

Allolactose binds to each of the four subunits of the LacI repressor which are assumed to be identical. The corresponding equilibrium constant has been measured as $\overline{K}_a = 1.7 \cdot 10^6 M^{-1}$ (27). Given a cell volume of $V_{cell} = 10^{-15} l$ the equilibrium constant can be written in terms of relative mass units as

$$K_a = \frac{\overline{K}_a}{mp_A \cdot N_A \cdot V_{cell}} = 1.5 \cdot 10^6 \frac{1}{\frac{g_A}{gdw}}.$$

LacZ synthesis

In our model, transcription occurs if either all three operator sites are repressor-free or if only O_2 is bound by a repressor molecule. The probability for transcription is given by the expression in Eq. (6). At full induction a maximal number of 5 LacZ tetramers can be produced per second (28) so that V_Z is given by

$$V_Z = 5\frac{mlc_Z}{s} \cdot mp_Z = 0.046\frac{g_Z}{gdw}\frac{1}{h}.$$

Conversion of lactose into allolactose and glucose/galactose

Using lactose as a substrate LacZ may either generate glucose and galactose to sustain growth or it may generate the inducer allolactose. Experiments have shown that at sufficiently low lactose concentrations both processes occur at approximately equal rates (29) that can be described by a Michaelis-Menten rate of the form

$$\bar{V}_{lac}[LacZ]\frac{[Li]}{\bar{K}_{lac} + [Li]} \tag{M4}$$

where $\bar{V}_{lac}$ and $\bar{K}_{lac}$ are given by $\bar{V}_{lac} = 32.6\ U/mg$ and $\bar{K}_{lac} = 2.53mM$ (30). Using that 1Unit (U) corresponds to the amount of substrate (in µmol) that can be converted by 1 mg of protein per minute we can rewrite $\bar{V}_{lac}$ in the form

$$\bar{V}_{lac} = 32.6\frac{60 \cdot 10^{-6} mol_L}{h \cdot 10^{-3} g_Z} \cdot m_Z = 907584\frac{mlc_L}{mlc_Z}\frac{1}{h}$$

or, in relative mass units, as

$$V_{lac} = \bar{V}_{lac}\frac{mp_L}{mp_Z} = 670\,\frac{\frac{g_L}{gdw}}{\frac{g_Z}{gdw}}\frac{1}{h}.$$

Similarly, rewriting the Michaelis-Menten constant $\bar{K}_{lac}$ in relative mass units yields

$$K_{lac} = \bar{K}_{lac} \cdot mp_A \cdot N_A \cdot V_{cell} = 0.0029\,\frac{g_L}{gdw}.$$

Conversion of allolactose into glucose and galactose

LacZ can also use allolactose as a substrate (30). In that case, glucose and galactose are the main products while the reverse reaction (formation of lactose) does not seem to occur at an appreciable rate. The dynamics of this reaction is also described by a Michaelis-Menten rate of the form

$$\bar{V}_{al}[LacZ]\frac{[Al]}{\bar{K}_{al} + [Al]} \qquad \text{(M5)}$$

with $\bar{V}_{al} = 49.6\ U/mg$ and $\bar{K}_{al} = 1.2mM$. Rewriting these parameters in terms of relative mass units yields

$$V_{al} = \bar{V}_{al}\frac{mp_A}{mp_Z} = 1019\,\frac{\frac{g_A}{gdw}}{\frac{g_Z}{gdw}}\frac{1}{h}$$

and

$$K_{al} = \bar{K}_{al} \cdot mp_A \cdot N_A \cdot V_{cell} = 0.0014\,\frac{g_A}{gdw}.$$

In Eqs. (M4) and (M5) we have neglected possible competition effects that may exist between the LacZ substrates, lactose and allolactose, as they do not seem to affect the results of our study. For example, assuming competitive inhibition as done by

Dreisigmeyer et al. (8) yields the same values for the estimated parameters Y, K_L and K_i as without competition.

Growth yield on lactose

For the *E. coli* strain NCM3722 You et al. reported a growth yield in minimal medium on lactose of $Y = 150\ gdw/mol$ or $Y \approx 0.44\ gdw/g_L$ (31). However, in our experiments lactose is co-utilized with succinate (Fig. S3) making it difficult to evaluate the contribution of lactose utilization to the total biomass production. Due to this uncertainty we left the growth yield Y as a free parameter to be estimated by comparing model predictions with experiments. In that way we obtained the value $Y \approx 0.092\ gdw/g_L$ which indicates that a substantial portion of the imported lactose is, again, excreted either in the form of lactose and allolactose (as described by k_e^-) or in the form galactose and glucose as observed in (22). Since the latter two metabolites are not explicitly considered in our model their excretion is effectively accounted for in the maintenance term $\sim(1-Y)$ in Eq. (10).

Parameter estimation

To estimate the three free parameters in our model, Y, K_L and K_i, we have used the freely available Data 2 Dynamics software package (32). The model was simultaneously fitted to the transient lactose induction curves shown in Fig. 2 as well as to the growth curves shown in Fig. S1. To compare model predictions with the induction curves we have assumed that the measured LacZ activity (A) is proportional to the LacZ concentration in the cell, i.e. $A = a_0 + a_1[LacZ]$, where a_0 accounts for basal LacZ activity due to measurement noise. We have estimated these parameters together with the two main model parameters above and obtained the values

$$a_0 = 0.08\frac{U}{g} \;\; and \;\; a_1 = 52\,\frac{U/g}{g_Z/gdw}$$

which have been used to generate the plots in Fig. 2. To relate our model predictions for the cell density to the measurements shown in Fig. S1 we have used the relation $1\;OD = 5 \times 10^{11}$ cells/l, i.e. $1\;OD$ corresponds to a cell density of $c = 0.15gdw/l$.

Computation of the two-parameter bifurcation diagram

The two-parameter bifurcation diagram in Fig. 3C has been computed using MATCONT – a freely available software package for numerical bifurcation analysis (33). To this end, we used the external lactose concentration (Le) and the LacI overexpression factor (ρ_I) as independent parameters. The latter can be introduced through the parameters α_i $(i = 1,2,3)$, $\hat{\alpha}_j$ $(j = 1,2)$ and κ_2 in the expression for P_S in Eq. (6). According to the mechanistic model described in (34) these parameters describe unary ($\alpha_1, \hat{\alpha}_1, \kappa_2$), binary ($\alpha_2, \hat{\alpha}_2$) and ternary ($\alpha_3$) repressor-operator interactions and are, thus, proportional to first, second and third power of the LacI concentration

$$\alpha_1, \hat{\alpha}_1, \kappa_2 \sim LacI_T, \;\; \alpha_2, \hat{\alpha}_2 \sim LacI_T^2, \;\; \alpha_3 \sim LacI_T^3.$$

Hence, we have multiplied $\alpha_1, \hat{\alpha}_1$ and κ_2 by ρ_I, α_2 and $\hat{\alpha}_2$ by ρ_I^2 and α_3 by ρ_I^3 to account for relative changes in the expression level of LacI repressor.

Strains, plasmids and growth media

Strains used in this study are the reporter strain AM1 (11), carrying an additional copy of the *lac* promoter region including all three operator sites and controlling the expression of a LacZ´-Gfp fusion protein. By transforming AM1 with the medium copy number plasmid (ColE1 origin) pRR48c (35) encoding *lacI*^{q} we obtained the strain DZ2 with strongly elevated *lacI* copy number. For low increase of LacI copy number, *lacI* including its own promoter was PCR amplified from chromosomal DNA of LJ110 (36) and fused into the low copy vector pCS26 (about 10 copies/cell) (37) using the Gibson assembly cloning kit from NEB (Ipswich, USA), thereby deleting the NotI fragment and hence the *lux* genes. This plasmid was transformed into AM1 giving rise to strain DZ3.

Strains were grown either in LB_0 medium (10g/l tryptone, 5 g/l yeast extract, 5 g/l NaCl) or in chemically defined phosphate buffered minimal medium (38) with 0.2 g/l succinate. DZ2 was grown in the presence of ampicillin (10 µg/ml) and DZ3 was grown in the presence of kanamycin (25 µg/ml).

Growth conditions and media for *lac* operon induction experiments

For determination of *lac* operon induction by enzymatic assay single colonies grown on LB_0 agar plates (10g/l tryptone, 5 g/l yeast extract, 5 g/l NaCl, 12 g/l agar) were inoculated for 3-5 h in LB_0 liquid medium. Precultures were diluted by 1:100 in minimal medium supplemented with 0.2% (w/v) succinate and cultivated in shake flasks overnight. The overnight cultures were washed 3 times with minimal medium without carbon source and were used to inoculate the main cultures with an initial optical density (OD) of 0.1 at 420nm (corresponding to about $5 \cdot 10^7$ cells/ml). After about 1 h of cultivation cell suspensions were induced by adding the corresponding lactose concentrations. Samples for ß-galactosidase assays and for determination of cell density as well as supernatants were taken every 30 min.

Cultivations for microscopy analysis were conducted similarly. To ensure that lactose concentrations were not significantly depleted at the end of the cultivations, these experiments were performed with very low initial cell densities (200-500 cells/ml). This resulted in very low cell numbers also at the end of the experiment. Cell numbers in this case were determined by plating culture aliquots on LB_0 plates and counting of the colonies grown. Lactose levels at the beginning and at the end of the experiments were measured to verify that the lactose concentration did not drop below 95% or 90% of the initial concentration (Fig. S2).

To investigate hysteresis effects, we additionally differentiated our overnight cultures in uninduced and preinduced precultures. Uninduced overnight cultures were incubated in minimal medium plus 0.2% (w/v) succinate. For preinduced overnight cultures lactose was added to 3 mM in addition to 0.2% (w/v) succinate. Overnight cultures were washed 3 times and finally inoculated as described above. Samples were taken at the time points indicated. To stop gene expression at the time point of harvest chloramphenicol was added to 25µg/ml.

Fluorescence Microscopy

To measure *lac* operon gene expression at the single cell level 15-50 ml from the cultures were harvested and centrifuged for 15 min at 4500 rpm and 4°C. The supernatant was discarded and the pellet was resuspended in the return flow thoroughly. For 50mL only about 20mL were removed and the remaining suspension was centrifuged again. The suspension was transferred into a microcentrifuge tube and centrifuged again for 10 min at 4°C and at maximum speed. The supernatant was discarded except for 50µl. The pellet was resuspended in the rest volume. Samples were applied to the microscope slides covered with 1% agarose and the fluorescence intensity was measured with an AxioImager M1 microscope equipped with an AxioCam MRm CCD Camera (Zeiss). Monochrome photographs were taken in the fluorescence channel (excitation: BP 470/40, beamsplitter: FT495, emission: BP 525/50) and with phase contrast. Cell boundaries were determined from the phase contrast images by using Axiovision software of Zeiss. The mask generated was used for measuring GFP fluorescence in the fluorescence image. Fluorescence values were determined as the average fluorescence of the whole cell in arbitrary units. For each experiment images of about 300 - 600 cells were collected. Images were analyzed using the Axiovison software of Zeiss.

To compare the stimulus-response curves depicted in Figs. 3A and 3D with the mean GFP levels computed from the fluorescence distributions in Fig. 4 we have assumed that the mean GFP level is linearly related to the LacZ concentration as

$$\langle GFP\rangle = g_0 + g_1 \frac{[LacZ] - [LacZ]_{min}}{[LacZ]_{max} - [LacZ]_{min}} \quad \text{(M6)}$$

where $[LacZ]_{min}$ ($[LacZ]_{max}$) denote the minimum (maximum) of the respective LacZ stimulus-response curve. The basal GFP level, g_0, as well as the dynamic range, g_1, were directly obtained from the measured average GFP levels leaving the overexpression factor ρ_I as the only free parameter for the fit in Fig. 5B. In that way we have obtained the following values Fig. 5A: $g_0 = 220\ a.u.$, $g_1 = 600\ a.u.$ and Fig. 5B: $g_0 = 92\ a.u.$, $g_1 = 78\ a.u.$.

Note that the basal GFP level is markedly different between AM1 and DZ2 ($g_0^{AM1}/g_0^{DZ2} \approx 2.4$) which partially explains the substantially higher dynamic range for AM1 ($g_1^{AM1}/g_1^{DZ2} \approx 7.7$). The remaining factor of ~ 3.2 indicates that there exist growth effects or other regulatory processes due to LacI overexpression that are not captured by our model.

ß-Galactosidase Assay

For measuring the ß-galactosidase activity cells were harvested by centrifugation and the pellet was resuspended in 50mM phosphate buffer (34 mM Na_2HPO_4, 16 mM NaH_2PO_4, pH 7.2). The OD at 650 nm was adjusted to ~ 0.2. Finally 3 aliquots were frozen at -20°C. The activity of ß-galactosidase was determined similar to Miller et al. (39). Cell suspensions were thawed on ice and 10µl of toluene was added to 500µl of sample. After an incubation time of 5 min at 37°C and vigorous shaking, 25µl of 20mM o–nitrophenyl-ß-

D-galactopyranoside (ONPG) was added to the mixture. The chemical reaction was stopped by the addition of 750µl 0.2 mM Na_2CO_3 as soon as the sample turned yellow and the reaction time was noted. To remove cell debris the sample was centrifuged for 10 min at 13000 rpm. Finally absorption at 420nm was measured against water. To calculate the ß-galactosidase activity we used the following equation:

ß-galactosidase activity [U/mg protein] = $[OD_{(420nm)} * V_A * 4] / [t * \varepsilon * d * A_p]$,

with OD_{420nm} as the absorbance at 420nm, OD_{650nm} as the absorbance at 650nm, V_A as the volume of the reaction mix [ml], t as the reaction time [min], ε as the extinction coefficient for ortho-Nitrophenolat (E_{420}=4500/M cm), d as the length of the light path and A_p as the amount of protein used. The amount of protein was estimated by determining the optical density at 650nm (1 OD at 650 nm corresponds to 0.25 mg/ml protein).

Determination of lactose and succinate concentrations

Lactose and succinate concentrations in the supernatants were measured by using appropriate enzyme kits (Lactose/Galactose Assay kit, Megazyme, Wicklow, Ireland; succinic acid kit, R-Biopharm AG, Darmstadt, Germany). Samples were prepared by centrifugation of 1 ml cell suspension at 13000 rpm and 4°C for 1 min. The supernatant was collected and frozen at -20°C. The measurements were carried out in microtiter plates according to the manufacturer’s descriptions.

Results

Model choice and model description

To study the effect of growth rate-dependent dilution on the induction of the *lac* operon and the emergence of bistability we employed a modified version of a model proposed by Narang and Pilyugin (5). The reasons for this choice are two-fold: First, the model has been formulated in such a way that it is readily applicable to describe experiments in growing cell cultures. Specifically, it naturally incorporates the dependence of the growth rate on the Lac enzyme concentrations due to LacY-mediated uptake of lactose and LacZ-mediated lactose metabolism. Second, to describe repressor-operator interactions the model also properly accounts for DNA-looping states such that the expression for the synthesis rate of the Lac enzymes may exhibit sufficient non-linearity to overcome the growth rate-dependent dilution effect and, thus, may potentially allow for bistability. One limitation of the Narang-Pilyugin model is that the conversion of lactose into biomass has been assumed to be independent of LacZ. Since inducer production and lactose utilization rely on the presence of LacZ we have included this dependence in our model which consists of the following 5 ordinary differential equations (cf. *Methods* for details)

$$\frac{d[Le]}{dt} = -\left(V_L \frac{[LacY][Le]}{K_L + [Le](1 + [Li]/K_i)} - k_e^- [Li]\right) \cdot c \qquad (1)$$

$$\frac{d[Li]}{dt} = V_L \frac{[LacY][Le]}{K_L + [Le](1 + [Li]/K_i)} - 2V_{lac} \frac{[LacZ][Li]}{K_{lac} + [Li]} - k_e^- [Li] - \left(\frac{1}{c}\frac{dc}{dt}\right)[Li] \qquad (2)$$

$$\frac{d[Al]}{dt} = V_{lac} \frac{[LacZ][Li]}{K_{lac} + [Li]} - V_{al} \frac{[LacZ][Al]}{K_{al} + [Al]} - k_e^- [Al] - \left(\frac{1}{c}\frac{dc}{dt}\right)[Al] \qquad (3)$$

$$\frac{d[LacZ]}{dt} = V_Z \cdot P_S - \left(\frac{1}{c}\frac{dc}{dt}\right)[LacZ] \qquad (4)$$

$$\frac{d[B]}{dt} = \mu_b + Y \cdot \left(V_{lac} \frac{[LacZ][Li]}{K_{lac} + [Li]} + V_{al} \frac{[LacZ][Al]}{K_{al} + [Al]} \right) - V_Z \cdot P_S - \left(\frac{1}{c} \frac{dc}{dt} \right) [B]. \qquad (5)$$

Here, all concentrations and parameters are expressed with respect to the cell dry weight (cf. Tables 1 and 2). Eq. (1) describes the LacY-mediated uptake of extracellular lactose (Le), inhibition of LacY due to inducer exclusion as well as efflux of internalized lactose (Li) due to leak fluxes (40). Both terms in Eq. (1) are proportional to the cell density (c). The factor of 2 in Eq. (2) accounts for the fact that the LacZ-mediated conversion of lactose into allolactose (Al) and biomass (B) occurs at about equal proportions (29). The last two terms in Eq. (2) describe dilution of intracellular lactose due to excretion (k_e^-) or cell growth. The second term in Eq. (3) accounts for the fact that allolactose also acts as a substrate for LacZ (30). The last two terms in Eq. (3) have a similar meaning as those in Eq. (2).

Table 1: Variable names and units

name	external lactose concentration	intracellular lactose concentration	intracellular allolactose concentration	intracellular LacZ concentration	cell density
symbol	$[Le]$	$[Li]$	$[Al]$	$[LacZ]$	c
unit	$\frac{g_L}{l}$	$\frac{g_L}{gdw}$	$\frac{g_A}{gdw}$	$\frac{g_Z}{gdw}$	$\frac{gdw}{l}$

gdw = cell dry weight ($3 \times 10^{-13} g$), in g_X the $X = L, A, Z$ indicates the species to which it refers

In Eq. (4),

$$P_S = \frac{1 + \frac{\kappa_2}{(1 + K_a[Al])^2}}{1 + \frac{\alpha_1}{(1 + K_a[Al])^2} + \frac{\hat{\alpha}_1 + \alpha_2}{(1 + K_a[Al])^4} + \frac{\hat{\alpha}_2 + \alpha_3}{(1 + K_a[Al])^6}} \qquad (6)$$

represents the probability for *lac* gene transcription (34), and V_Z denotes the maximal rate of protein synthesis summarizing the effects of both transcription and translation. Here, changes of the gene copy number (as a function of the growth rate) are not considered as they are negligible for the range of growth rates considered in our study (41). The expression for P_S has been derived under the assumption that transcription can occur if either all operator sites are repressor-free or if only O_2 is bound by a LacI repressor. This is consistent with the finding that LacI binding to O_2 has essentially no effect on the transcriptional activity (3). In Eq. (6), K_a denotes the equilibrium constant for inducer-repressor binding whereas the α_i account for all operator-repressor states where either one (α_1), two (α_2) or all three (α_3) operator sites are occupied by LacI. The parameter $\hat{\alpha}_1$ describes operator-repressor states where one repressor molecule is simultaneously bound to any two of the three operator sites forming a DNA loop. Similarly, $\hat{\alpha}_2$ accounts for operator-repressor states where two repressor molecules are bound to any two of the three operator sites and, in addition, one of the repressor molecules forms a DNA loop with the remaining free operator site. Finally, $\kappa_2 = K_2 \cdot LacI_T$ denotes the equilibrium constant for LacI binding to the O_2 site rescaled by the total repressor concentration ($LacI_T$). Also, note that $\kappa_2 < \alpha_1 = \kappa_1 + \kappa_2 + \kappa_3$ where $\kappa_i = K_i \cdot LacI_T$ denote the rescaled equilibrium binding constants with respect to operator site O_i. Further details concerning the derivation of the expression in Eq. (6) can be found in Ref. (34).

The dynamics of LacY is not explicitly modeled since LacY and LacZ are cotranslated from the same polycistronic mRNA. Measurements of the respective translation rates have shown that, to a good approximation, the two proteins are produced in a fixed ratio of 2:1 (LacY:LacZ) (28). Assuming that LacY and LacZ are not actively degraded but only diluted by cell growth their concentrations can be related via

$$[LacY] = 2\frac{mp_Y}{mp_Z}[LacZ] \tag{7}$$

where mp_Y and mp_Z denote the relative mass fractions of LacY and LacZ with respect to the total cell dry weight, respectively (cf. Table S1).

Eq. (5) describes the production of biomass (B) other than that contributed by Li, Al and $LacZ$. Since the synthesis of LacZ is already accounted for in Eq. (4) a corresponding term has to be subtracted from the total synthesis rate of biomass. The first term in Eq. (5) describes biomass production due to growth on succinate whereas Y denotes the growth yield on lactose. Since all intracellular concentrations are expressed in terms of relative mass units (g/gdw) the total cell dry weight is determined by the relation

$$[Li] + [Al] + [LacZ] + [B] = 1. \tag{8}$$

By adding up Eqs. (2) – (5) and using Eq. (8) one obtains an equation for the cell density which reads

$$\frac{dc}{dt} = \mu \cdot c \tag{9}$$

where the specific growth rate μ is given by

$$\begin{aligned} \mu = \mu_b + V_L \frac{[LacY][Le]}{K_L + [Le](1 + [Li]/K_i)} - k_e^-([Li] + [Al]) \\ - (1 - Y)\left(V_{lac}\frac{[LacZ][Li]}{K_{lac} + [Li]} + V_{al}\frac{[LacZ][Al]}{K_{al} + [Al]}\right). \end{aligned} \tag{10}$$

Thus, in the absence of lactose in the external medium, the specific growth rate is determined by the basal growth rate on succinate. However, when lactose is present μ is increased by the net rate of lactose uptake which is given by the lactose import rate reduced by losses due to excretion and maintenance (5). Note that since $\mu \sim [LacY] \sim [LacZ]$ the total dilution rate of the Lac enzymes is $\mu \cdot [LacZ] \sim [LacZ]^2$ which is the growth rate-dependent dilution effect mentioned above.

Parameter estimation

To validate the model described by Eqs. (1) – (10) we fixed all but three parameters at their experimentally known values (cf. Table 2). For the remaining three parameters (the growth yield on lactose (Y), the half-saturation constant for lactose import (K_L) and the inhibition constant for LacY (K_i)) either no literature value has been available or a large uncertainty existed in its value (cf. *Methods*). To estimate these parameters for our *E. coli* strain (AM1, see below) we used cells growing exponentially in minimal medium on succinate ($\mu_b = 0.33/h$) and applied increasing amounts of lactose. The resulting transient changes of LacZ activity were measured together with the growth rate and subsequently used to fit the model (Fig. 2 and Fig. S1). The estimated parameter values for Y, K_L and K_i are listed together with those of the fixed parameter values in Table 2. Note that the LacY inhibition constant K_i is one order of magnitude smaller than the Michaelis-Menten constants (K_{lac} and K_{al}) for the LacZ-catalyzed reactions indicating that the negative feedback due to inducer exclusion becomes effective well before LacZ is saturated. The other two parameters are discussed in the *Methods* section.

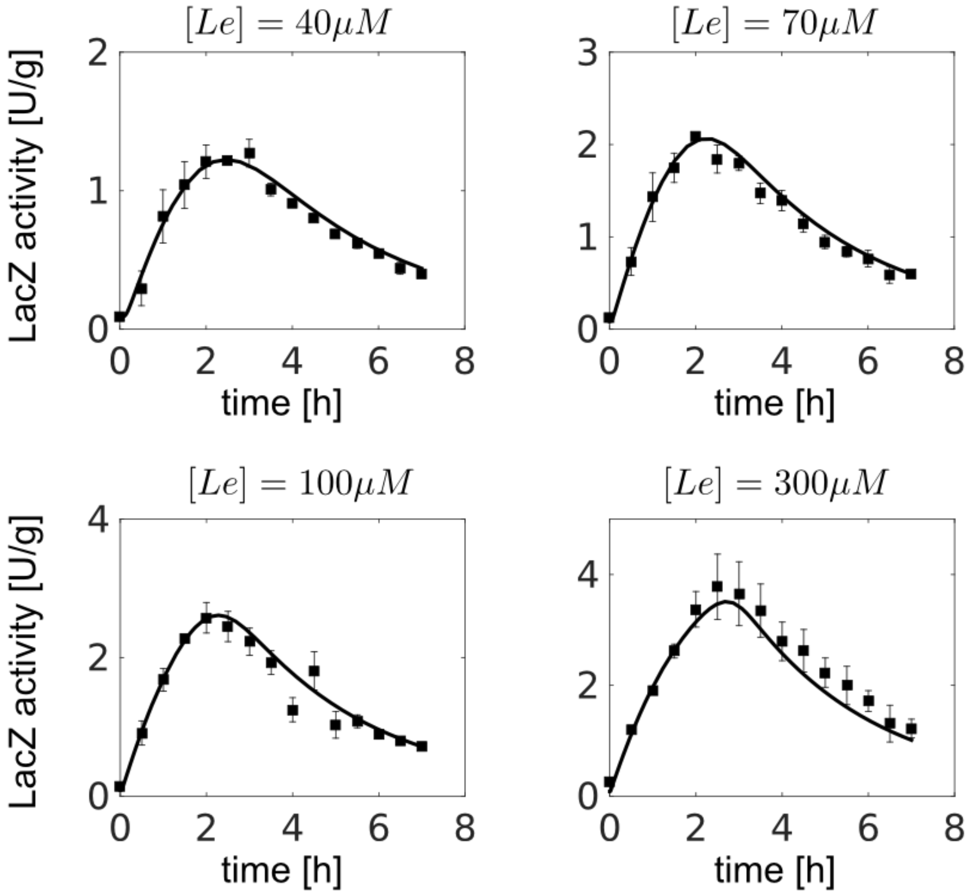

Fig. 2: Parameter estimation. Cells grown on succinate are induced with increasing amounts of lactose and the transient change in LacZ activity has been measured (symbols). Error bars represent sd from 3 independent experiments. The solid lines represent the best (least square) fit of the model equations (Eqs. 1-6). The corresponding parameter values are shown in Table 2.

Table 2: Model parameters

name	value	reference	name	value	reference
V_L	$1271 \frac{g_L/gdw}{g_Y/gdw}\frac{1}{h}$	(19)	κ_2	0.38	(34)
K_L	$0.68\ g_L/l$ $(\approx 2mM)$	estimated	α_1	31	
K_i	$0.00013\ \frac{g_L}{gdw}$	estimated	$\hat{\alpha}_1$	1420	
V_{lac}	$670 \frac{g_L/gdw}{g_Z/gdw}\frac{1}{h}$	(30)	α_2	19	
K_{lac}	$0.0029 \frac{g_L}{gdw}$		$\hat{\alpha}_2$	322	

V_{al}	$1019 \frac{g_A/gdw}{g_Z/gdw} \frac{1}{h}$		α_3	3	
K_{al}	$0.0014 \frac{g_A}{gdw}$		Y	$0.092 \frac{g_L}{gdw}$	estimated
V_Z	$0.046 \frac{g_Z/gdw}{h}$	(28)	k_e^-	$60 \frac{1}{h}$	(21)
K_a	$1.5 \cdot 10^6 \frac{1}{g_A/gdw}$	(27)	μ_b	$0.33 \frac{1}{h}$	measured

g_X/gdw denotes gram of species $X = L, A, Y, Z$ per gram dry weight (cf. Table 1).

The natural lactose utilization system exhibits a non-monotonic response curve

Having a well-parameterized model we were first interested whether the induction of the *lac* operon would be predicted to occur in a monostable or in a bistable manner. As Fig. 3A shows the stimulus-response curve of LacZ induction is monostable. In addition, it exhibits a pronounced maximum at intermediate lactose concentrations. To understand the origin of this maximum at the level of our computational model one has to consider that lactose is used for both LacZ induction and cell growth, and that the relative contributions of these two processes, which determine the steady state level of LacZ, vary depending on the external lactose concentration. Indeed, at low inducer concentrations positive changes in the allolactose concentration mainly increase the LacZ synthesis rate while the specific growth rate remains approximately constant (Fig. 3B). As a result, the LacZ activity rises as a function of the external lactose concentration. However, as more lactose is pumped into the cell all LacI binding sites eventually become occupied by inducer molecules so that the LacZ synthesis rate saturates. Any additional allolactose is either excreted or converted into glucose and galactose which then leads to an increased growth rate. This line of reasoning is supported by direct measurement of the specific growth rate at different lactose concentrations in the medium (Fig. S2A). Hence, at high inducer concentrations the dilution term in Eq. (4) becomes dominant so that increasing the extracellular lactose concentration beyond the point, where the intracellular allolactose concentration becomes saturating for LacZ synthesis, leads to a reduction of LacZ activity and, thereby, to a maximum in the induction curve. Note that such a non-monotonic behavior would not be expected to occur if the *lac* operon is induced with gratuitous inducers such as TMG or IPTG as they do not affect the growth rate in our model.

To test these predictions we analyzed *lac* operon induction in single cells. To this end, we employed the GFP reporter strain AM1 (11) which contains one additional copy of the *lac* promoter-operator region (cf. Fig. 1). To keep the O2 binding site (in addition to O1 and O3) the first codons of *lacZ* were fused to *gfpmut*3.1, resulting in a LacZ-GFP fusion protein, which has been integrated at the attachment site of phage80. As only one additional promoter-operator region was inserted we regard *lac* operon regulation to be basically unchanged in AM1 compared to the wildtype.

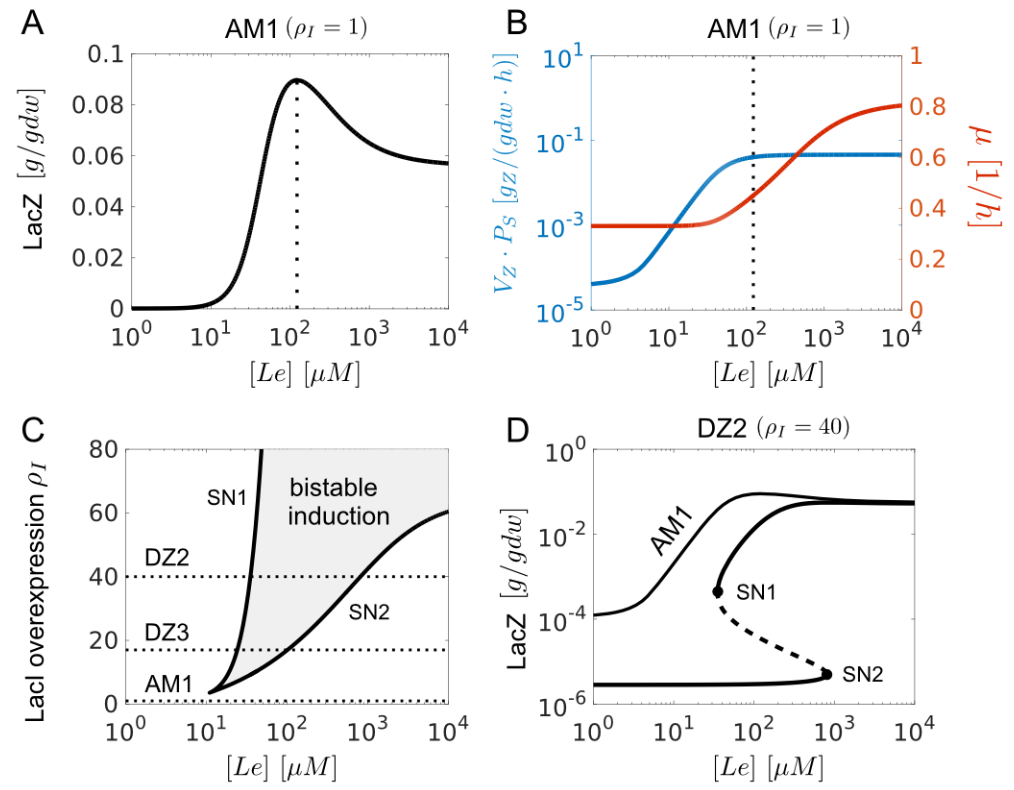

Fig. 3: Model predictions: Non-monotonic response and bistability. (A) For the wildtype strain (AM1) the LacZ induction curve is predicted to occur in a monostable manner, but it exhibits a pronounced maximum at $[Le] \approx 120\mu M$ (dotted line). (B) Near the dotted line (same as in A) the LacZ synthesis rate (solid line, Eq. 6) saturates while the specific growth rate (dashed line, Eq. 7) begins to increase which rationalizes the occurrence of the maximum in A. (C) Two-parameter bifurcation diagram depicting the region (shaded area) where *lac* operon expression is predicted to occur in a bistable manner. (D) Sample stimulus-response curve at $\rho_I = 40$ exhibits two stable steady states (solid lines) separated by two saddle node bifurcations (SN1 and SN2) from an unstable steady state (dashed line) at intermediate lactose concentrations. For comparison the stimulus-response curve from (A) is shown as thin solid line (note the logarithmic y-scale in D).

The AM1 strain was tested for induction of the *lac* operon after growth in batch cultures with 0.2% succinate by adding varying levels of lactose ranging from 0 to 2mM. We have chosen succinate as a background substrate for two reasons: First, it allows for growth of both induced as well as uninduced cells independent of the induction status of the *lac* operon. Second, succinate does not interfere significantly with *lac* operon induction as it does not elicit catabolite repression or inducer exclusion. We have also checked that both substrates are taken up concurrently (Fig S3). To ensure that the lactose concentration in the medium would remain approximately constant during the subsequent growth phase cells were inoculated to a very low cell density (≤10^{-5} OD) similar as done in Ref. (10). In this way we could achieve nearly steady state conditions for up to 17h of growth (Fig. S2B). The minimal length of the growth phase has been chosen based on model simulations suggesting that *lac* induction would reach a steady state after 5-10h depending on the lactose concentration in the medium. At the end of the growth phase (10h-17h) cells were sampled and analyzed by fluorescence microscopy.

As shown in Fig. 4 (AM1) the resulting single-cell GFP distributions were unimodal for all lactose concentrations tested which confirms previous reports by other groups (10, 42). As the extracellular lactose concentration is increased the population-averaged GFP level first rises gradually up to a maximum at $[Le] \approx 150\mu M$ from which it gradually declines as $[Le]$ is further increased. Assuming a linear relationship between LacZ activity and GFP expression the measured average GFP levels can be mapped to the stimulus-response curve depicted in Fig. 3A (cf. *Methods*). The resulting curve (Fig. 5A) has a similar shape as the measured GFP levels supporting our model prediction that the LacZ activity exhibits a maximum at intermediate lactose concentrations.

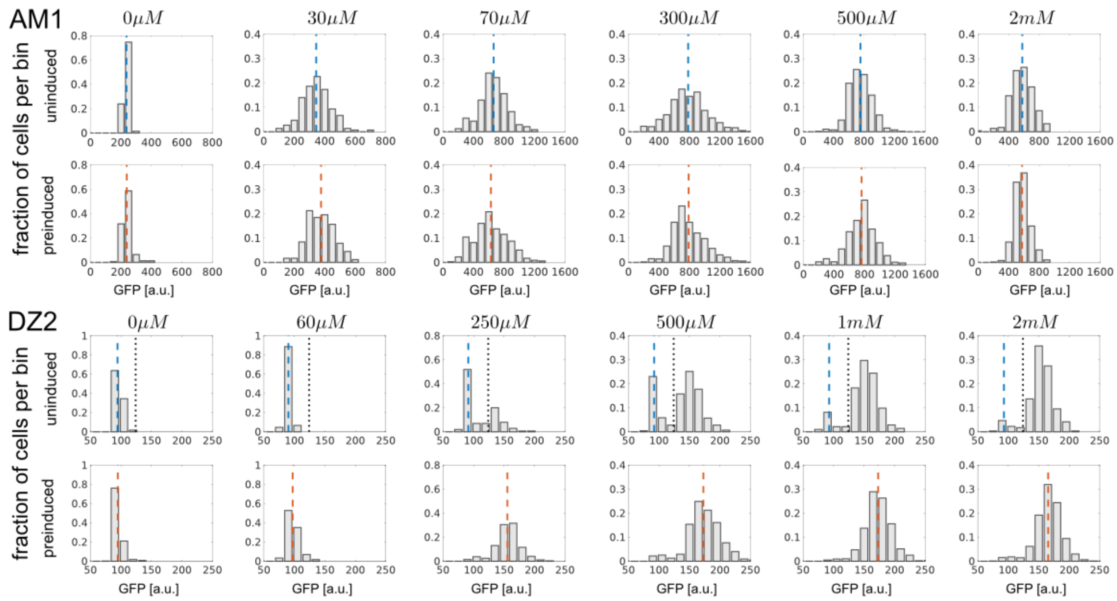

Fig. 4 Fluorescence distributions of AM1 and DZ2 after 17h steady state growth. Lactose concentrations are indicated above the panels. For AM1 GFP distributions are unimodal for all concentrations while DZ2 (uninduced) exhibits bimodal distributions in the range between 250μM-2mM. Uninduced (preinduced) cells were grown in the presence of 0.2% succinate (3mM lactose) before they were resuspended into medium with defined lactose concentration as indicated above the panel. For AM1 (preinduced, uninduced) and DZ2 (pre-induced) the long-dashed line indicates the mean GFP level of the total population. For DZ2 (uninduced) the short-dashed line indicates the mean GFP level of “off” cells which have remained uninduced after 17h. The dotted line marks the threshold GFP level for “off” cells. Incubation time for AM1 (500μM and 2mM) was 10h.

To exclude hysteresis effects we have repeated the induction experiments with preinduced precultures. To this end overnight cultures were grown in the presence of 3mM lactose before they were washed, diluted and resuspended into fresh medium containing the same lactose concentration as used before. However, we could not observe any qualitative difference between precultures grown in the presence or in the absence of lactose both at the level of the GFP distributions (Fig. 4, AM1) as well as for the average GFP levels (Fig. 5A). Together these observations support previous results according to which the natural lactose utilization system operates in the monostable regime.

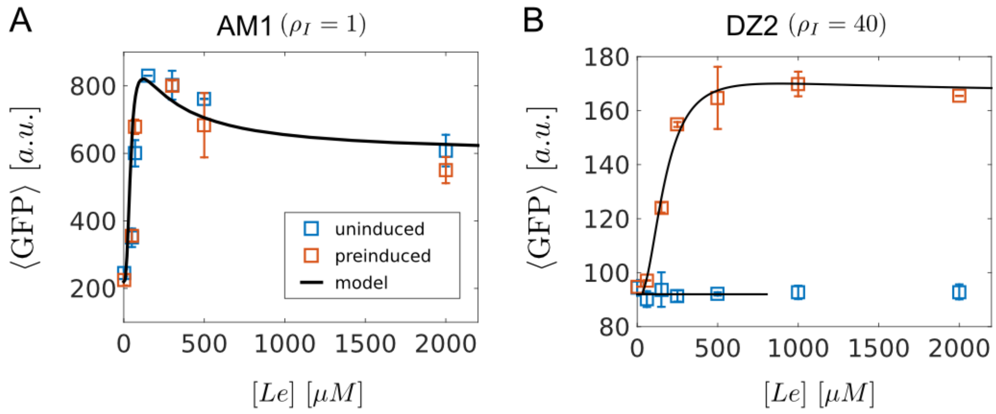

Fig. 5: Comparison of stimulus-response curves with mean GFP expression levels. In (A) symbols denote mean GFP levels as indicated by the lomg-dashed lines in Fig. 4 (AM1). In (B) circles correspond to mean GFP levels as indicated by the lomg-dashed lines in Fig. 4 (DZ2, preinduced). In contrast square symbols denote the mean GFP levels computed from the “off” cell population marked by short- dashed lines in Fig. 4 (DZ2, uninduced). Model predictions (solid lines, same as in Fig. 3A and 3D) were linearly scaled according to Eq. (M6) (cf. *Methods*). Error bars represent sd from at least 2 independent experiments.

The natural lactose utilization system operates close to a bistable region

The finding that the LacZ induction curve is monostable indicates that in the natural lactose utilization system the cooperativity of repressor-operator interactions due to DNA-looping is not sufficient to overcome the attenuating effect of the growth rate-dependent dilution of the Lac enzymes (5). However, it has been argued that the cooperativity generated by DNA-looping can be substantially increased through overexpression of LacI repressor (34). In addition, *lacI* overexpression reduces the basal LacZ expression level which, according to the Savageau design principle (6), should also favor the emergence of bistability. To test these predictions we first computed a two-parameter bifurcation diagram with the external lactose concentration on the x-axis and the fold change overexpression level of LacI on the y-axis (see Methods). The resulting diagram indicates that the natural *lac* system ($\rho_I = 1$) operates close to a bistable region (Fig. 3C, shaded region) which extends from $\rho_I \gtrsim 3.5$ and $[Le] \gtrsim 10\mu M$ towards higher lactose concentrations. For low overexpression factors the bistable region is extremely narrow making it unlikely to observe bistability experimentally. However, as ρ_I increases beyond 20 the bistable region substantially increases as well. For example, at $\rho_I = 40$ two stable steady states coexist in the region $35\mu M \leq [Le] \leq 811\mu M$ (Fig. 3D). As expected due to the increased *lac* gene repression the basal LacZ expression level is substantially reduced compared to AM1. However, the non-monotonic behavior of the stimulus-response curve is still visible in the upper stable branch of the bistable induction curve, albeit to a much lesser extent.

To experimentally test whether increasing the repressor level would lead to a bistable *lac* operon induction we transformed AM1 with plasmid pRR48. This plasmid carries the *lacI^q* allel (35) and the ColE1 replicon (about 20-50 copies per cell) and hence is expected to elevate the LacI copy number substantially. In contrast to AM1 no induction could be achieved with lactose concentrations below 250μM while the same concentration was sufficient to fully induce AM1 (Fig. 4, AM1). In addition, the dynamic range of *lac* operon expression as well as the maximal growth rate at saturating lactose concentrations appeared to be reduced (cf. Table 3). Comparable results were obtained by Bhogale et al. (43) for induction of a similar strain with TMG. For lactose concentrations equal to or larger than $250\mu M$ we observed history-dependent induction behavior as it typically occurs in connection with bistability (Fig. 4, DZ2). While cells from precultures grown in the absence of lactose exhibited bimodal distributions at in the range between $250\mu M - 2mM$ the distributions of cells from precultures grown in the presence of lactose were found to be unimodal. Moreover, as the lactose concentration is increased the fraction of cells in the uninduced state (below the dotted line) gradually decreased while, at the same time, the fraction of induced cells increased accordingly.

Table 3: Comparing AM1 and DZ2

	AM1	**DZ2**
specific growth rate μ at $[Le] = 0\mu M$	$0.33/h$	$0.2/h$
specific growth rate μ at highest lactose concentration	$0.81/h$ ($[Le] = 4mM$)	$0.42/h$ ($[Le] = 2mM$)
dynamic range ($< \Delta GFP >$)	2.73	0.85

$< \Delta GFP > = (< GFP >_{max} - < GFP >_{min}) / < GFP >_{min}$ (cf. Eq. M6 in *Methods*). Growth rates were interpolated from cell numbers (determined by plating) at the beginning and at the end of a 17h experiment.

We expected that the history-dependent effects at the distribution level would result in a hysteresis curve similar to that in Fig. 3D. We reasoned that the mean GFP level computed from preinduced precultures should coincide with the upper stable branch of the hysteresis curve while the lower stable branch should be identified with the mean GFP level of “off” cells (Fig. 4, DZ2, uninduced), i.e. cells which have not yet been induced after 17h. One inherent uncertainty of such a procedure comes from the fact that the exact location of the bifurcation points (denoted by SN1 and SN2 in Fig. 3D) cannot be directly inferred from the GFP distributions in Fig. 4. However, one would expect that the left bifurcation point (SN1) lies below the concentration for which bimodal distributions first appear ($[Le] = 250\mu M$ in our case). The reason is that the transition to the induced state is a stochastic process driven by fluctuations in the operator occupancy of the LacI repressor (43, 44). To become induced fluctuations have to drive the cells beyond the unstable branch of the hysteresis curve (Fig. 3D, dashed line) which typically occurs only if the inducer concentration is sufficiently increased beyond the left bifurcation point (10). Also, the location of bifurcation points might be shifted in the presence of fluctuations (45). For example, in the case of an auto-activating gene circuit it has been shown that noise has a stabilizing effect on the lower stable steady state so that the right bifurcation point is moved towards higher values of the bifurcation parameter (46). Applied to our situation this suggests that the location of the right bifurcation point (SN2) is actually below 1-2mM assuming that the range of bistability as predicted by our deterministic model is narrower than that observed experimentally.

To compare the hysteresis curve computed from the model with the mean GFP levels (Fig. 5B) we assumed a linear relation between LacZ activity and GFP expression leaving the overexpression factor ρ_I as the only free parameter (cf. *Methods*). While the shape of the upper stable branch of the hysteresis curve was largely insensitive to the particular value of ρ_I the extent of the bistable region was highly variable extending from $31\mu M \leq [Le] \leq 353\mu M$ at $\rho_I = 30$ to $39\mu M \leq [Le] \leq 2000\mu M$ at $\rho_I = 50$ (Fig. S4). Hence, both values would be consistent with the expectation that the left bifurcation point lies below $[Le] = 250\mu M$. However, as ρ_I increases the maximum in the response curve becomes less pronounced. Best agreement with the upper stable branch is obtained for $\rho_I = 40$ (Fig. 5B). Here, the response curve exhibits a mild decline at high lactose concentrations while the right bifurcation point (SN2) lies below 1mM. Note, however, that the estimate of ρ_I is only approximate and might be affected by further factors, e.g. a spatially inhomogeneous distribution of LacI repressor inside the cell (47).

A lower overexpression factor leads to a down-shift of the bistable regime

According to the two-parameter bifurcation diagram depicted in Fig. 3C lowering the LacI overexpression factor ρ_I should narrow the bistable region and shift it towards lower lactose concentrations. To test this model prediction we constructed a second strain denoted by DZ3. In that strain *lacI* (with its natural promoter) was cloned onto a low copy number plasmid, so that (compared to DZ2) a moderate elevation of the LacI copy number of 5-10 was expected. According to Fig. 3C, a 10-fold increase of the LacI copy number should result in bistability in the range $20\mu M \leq [Le] \leq 40\mu M$. However, at such low concentrations we have only observed unimodal fluorescence distributions independent of the growth history of the population. Instead, bimodal distributions were observed for uninduced cells in the range between $80\mu M \leq [Le] \leq 100\mu M$ (Fig. S4). The corresponding value for the LacI overexpression factor $\rho_I \approx 17$ (cf. Fig. 3C) indicates that in DZ3 the LacI copy number was slightly larger (~ 2x) than expected. Together, these results support the model prediction that lowering the overexpression factor narrows the bistable regime and shifts it towards lower inducer concentrations.

Discussion

The all-or-none induction of the *E. coli lac* operon has been a paradigmatic example for bistability in gene regulatory networks for many decades. However, so far bistability has been experimentally demonstrated only for induction with gratuitous inducers such as TMG (9, 10, 48) or IPTG (11, 12), but not for induction with the natural inducer lactose. In fact, based on theoretical analysis of the *lac* circuit architecture Savageau argued that bistability is unlikely to occur in the natural lactose utilization system, but that overexpression of the LacI repressor would favor the emergence of bistability (6).

In the present study we have tested and confirmed this prediction by combining single cell analysis with deterministic computational modeling. To this end we analyzed *lac* operon induction by lactose in *E. coli* cells, both in a wildtype-derived GFP-containing reporter strain (AM1) and in mutants overexpressing the LacI repressor to different extents (DZ2 and DZ3). In this sense our experiments can be viewed as opposite to those conducted by Ozbudak et al. who showed that TMG-induced *lac* operon expression can be driven from a bistable into a monostable regime by successive dilution of LacI repressor (10). Guided by the computational model our results support the view that *lac* operon induction in the wildtype strain is graded (monostable) rather than all-or-none (bistable) which is consistent with the Savageau design principle as well as with previous experimental analysis of lactose-induced *lac* operon expression in *E. coli* (42).

In contrast, GFP expression in DZ2 and DZ3 was bimodal after 17h of steady state growth. According to our model the range of lactose concentrations over which bistability is predicted to occur should become larger and shift towards higher lactose concentrations as the LacI overexpression factor increases. Qualitatively, this is indeed what we have observed: For DZ2 (strong *lacI* overexpression) we obtained bimodal distributions in the range of lactose concentrations between $250\mu M - 2mM$ while DZ3 (moderate *lacI* overexpression) yielded bimodal distributions in the range between $80\mu M - 100\mu M$. However, especially in DZ2 both the growth rate at saturating lactose levels as well as the dynamic range of GFP expression were substantially reduced compared to AM1 (cf. Table 3). In addition, induction by lactose appears to be a fast process occurring within only ~2 cell generations (Fig. 2). Hence, at least at the conditions tested, with succinate as an alternative carbon source, one would not expect a significant growth advantage for *E. coli* to operate the lactose utilization system in the bistable regime following, for example, a bet-hedging strategy. The latter is believed to be beneficial if the response rate of a system is comparable to or lower than the rate with which environmental changes occur (49).

Possible mechanisms behind the non-monotonic response

Even though the LacZ induction curve of AM1 is monostable it exhibits a pronounced maximum at intermediate lactose concentrations around $150\mu M$ (Fig. 3A and Fig. 5A). Interestingly, a similar maximum in the response curve of LacZ expression has recently been observed by Afroz et al. (42) although no attempt has been made to explain this effect. Our model-based analysis suggests that the maximum arises from the saturation of LacI repressor by allolactose at low inducer concentrations and the growth rate-dependent dilution effect which provides a negative feedback at high inducer concentrations (Fig. 3B). Clearly, such a non-monotonic response cannot occur with gratuitous inducers such as TMG and IPTG as these do not increase the growth rate. To obtain a maximum at intermediate lactose levels one also has to require that the inducer concentration, which leads to saturation of the LacI repressor, should be low enough not to saturate the catabolic enzymes such that increasing the lactose level beyond the repressor saturation point can still increase the growth rate – a condition which seems to be satisfied for the lactose utilization system. Moreover, it seems likely that this condition also holds in other repressor-mediated sugar uptake systems as the number of repressor molecules is typically much lower than that of the catabolic enzymes.

The Lac protein expression maximum might also be reasoned in the connection between lactose metabolism and the glucose-PTS which provides an alternative negative feedback mechanism to reduce *lac* gene expression at high lactose concentrations. Indeed, when lactose uptake rates are low only small amounts of intracellular glucose are produced from the LacZ-mediated cleavage of lactose into galactose and glucose. However, this small amount of glucose might not be sufficient to provoke significant dephosphorylation of the PTS proteins. The situation becomes different at $[Le] \approx 150\mu M$ when enough allolactose is produced to fully saturate LacI so that further increases of the extracellular lactose concentration lead to an increased production of intracellular glucose which can be phosphorylated by the PTS (50, 51). Concomitantly, the concentration of dephosphorylated $EIIA^{Glc}$ increases, thereby mediating inducer exclusion through inhibitive binding to LacY (23). The same effect will also promote catabolite repression by reducing the availability of the cAMP.CRP complex as phosphorylated $EIIA^{Glc}$ is necessary to activate adenylate cyclase (13). In our model we have only considered inducer exclusion as the more dominant effect in downregulating *lac* gene expression at high inducer concentrations (23, 24). However, the maximum in the LacZ response curve persists even in the absence of inducer exclusion ($K_i \rightarrow \infty$) suggesting that both inducer exclusion and catabolite repression are not necessary to explain the occurrence of the maximum.

At present we can only speculate about the physiological significance of the observed maximum in the Lac enzyme expression. An obvious purpose would be to avoid unnecessary LacZ and LacY synthesis when extracellular lactose levels become too high and hence to balance lactose uptake rates with central metabolism. In this respect it is interesting to note that a similar maximum in the induction curve has been observed for growth on N-acetylglucosamine, whose uptake is also mediated by a PTS (42). In contrast, uptake of non-PTS substrates (such as galactose) exhibited a monotonous induction curve, which may suggest that the PTS-mediated feedback on the expression of catabolic enzymes might be a general mechanism to limit the expression of these enzymes at high substrate concentration.

Author contributions

DZ performed and evaluated wetlab experiments. DS was involved in model setup and data analysis. RS designed and performed the modeling work and wrote the manuscript. KB designed and performed wetlab experiments and wrote the manuscript.

Acknowledgements

D. Zander and the experimental work have been funded by the Deutsche Forschungsgemeinschaft through the priority program 1617.

We thank Andrea Focke for excellent technical assistance.

References

1. Mueller-Hill, B. 1996. The lac operon: A short history of a genetic paradigm. Berlin: deGruyter.
2. Adhya, S. 1996. The lac and gal operons today. In: Lin ECC, AS Lynch, editors. Regulation of gene expression in Escherichia coli. Boston: Chapman & Hall. pp. 181–200.
3. Oehler, S., E.R. Eismann, H. Krämer, and B. Müller-Hill. 1990. The three operators of the lac operon cooperate in repression. EMBO J. 9: 973–9.
4. Griffith, J.S. 1968. Mathematics of Cellular Control Processes: II. Positive feedback to one gene. Theor. Biol. 20: 209–260.
5. Narang, A., and S.S. Pilyugin. 2008. Bistability of the lac operon during growth of Escherichia coli on lactose and lactose+glucose. Bull. Math. Biol. 70: 1032–64.
6. Savageau, M.A. 2011. Design of the lac gene circuit revisited. Math. Biosci. 231: 19–38.
7. van Hoek, M.J.A., and P. Hogeweg. 2006. In silico evolved lac operons exhibit bistability for artificial inducers, but not for lactose. Biophys. J. 91: 2833–43.
8. Dreisigmeyer, D.W., J. Stajic, I. Nemenman, W.S. Hlavacek, and M.E. Wall. 2008. Determinants of bistability in induction of the Escherichia coli lac operon. IET Syst. Biol. 2: 293–303.
9. Novick, A., and M. Weiner. 1957. ENZYME INDUCTION AS AN ALL-OR-NONE PHENOMENON. Proc. Natl. Acad. Sci. U. S. A. 43: 553–66.
10. Ozbudak, E.M., M. Thattai, H.N. Lim, B.I. Shraiman, and A. Van Oudenaarden. 2004. Multistability in the lactose utilization network of Escherichia coli. Nature. 427: 737–

40.

11. Marbach, A., and K. Bettenbrock. 2012. lac operon induction in Escherichia coli: Systematic comparison of IPTG and TMG induction and influence of the transacetylase LacA. J. Biotechnol. 157: 82–8.
12. Maloney, P.C., and B. Rotman. 1973. Distribution of suboptimally induces -D-galactosidase in Escherichia coli. The enzyme content of individual cells. J. Mol. Biol. 73: 77–91.
13. Postma, P.W., J.W. Lengeler, and G.R. Jacobson. 1993. Phosphoenolpyruvate:carbohydrate phosphotransferase systems of bacteria. Microbiol. Rev. 57: 543–94.
14. Kuhlman, T., Z. Zhang, M.H. Saier, and T. Hwa. 2007. Combinatorial transcriptional control of the lactose operon of Escherichia coli. Proc. Natl. Acad. Sci. 104: 6043–6048.
15. Yildirim, N., and M.C. Mackey. 2003. Feedback regulation in the lactose operon: a mathematical modeling study and comparison with experimental data. Biophys. J. 84: 2841–51.
16. Santillán, M., M.C. Mackey, and E.S. Zeron. 2007. Origin of bistability in the lac Operon. Biophys. J. 92: 3830–42.
17. van Hoek, M., and P. Hogeweg. 2007. The effect of stochasticity on the lac operon: an evolutionary perspective. PLoS Comput. Biol. 3: e111.
18. Booth, I.R., W.J. Mitchell, and W.A. Hamilton. 1979. Quantitative analysis of proton-linked transport systems. The lactose permease of Escherichia coli. Biochem. J. 182: 687–96.
19. Wright, J.K., and P. Overath. 1984. Purification of the lactose:H+ carrier of Escherichia coli and characterization of galactoside binding and transport. Eur. J. Biochem. 138: 497–508.
20. Wright, J.K., I. Riede, and P. Overath. 1981. Lactose carrier protein of Escherichia coli: interaction with galactosides and protons. Biochemistry. 20: 6404–15.
21. Kepes, A. 1960. Kinetic studies on galactoside permease of Escherichia coli. Biochim. Biophys. Acta. 40: 70–84.
22. Huber RE, Lytton J, F.E. 1980. Efflux of beta-galactosidase products from Escherichia coli. J. Bacteriol. 141: 528–33.
23. Inada, T., K. Kimata, and H. Aiba. 1996. Mechanism responsible for glucose-lactose diauxie in Escherichia coli: challenge to the cAMP model. Genes Cells. 1: 293–301.
24. Hogema, B.M., J.C. Arents, R. Bader, K. Eijkemans, T. Inada, H. Aiba, and P.W. Postma. 1998. Inducer exclusion by glucose 6-phosphate in Escherichia coli. Mol. Microbiol. 28: 755–65.
25. Seok, Y., J. Sun, H. Kaback, and A. Peterkofsky. 1997. Topology of allosteric regulation of lactose permease. Proc. Natl. Acad. Sci. 94: 13515–9.
26. Sondej, M., A. Weinglass, A. Peterkofsky, and H. Kaback. 2002. Binding of enzyme IIAGlc, a component of the phosphoenolpyruvate:sugar phosphotransferase system, to the Escherichia coli lactose permease. Biochemistry. 41: 5556–65.
27. Barkley, M., A. Riggs, A. Jobe, and S. Burgeois. 1975. Interaction of effecting ligands

with lac repressor and repressor-operator complex. Biochemistry. 14: 1700–12.

28. Kennell, D., and H. Riezman. 1977. Transcription and translation initiation frequencies of the Escherichia coli lac operon. J. Mol. Biol. 114: 1–21.

29. Huber, R.E., G. Kurz, and K. Wallenfels. 1976. A quantitation of the factors which affect the hydrolase and transgalactosylase activities of beta-galactosidase (E. coli) on lactose. Biochemistry. 15: 1994–2001.

30. Huber, R.E., K. Wallenfels, and G. Kurz. 1975. The action of beta-galactosidase Escherichia coli on allolactose. Can. J. Biochem. 53: 1035–8.

31. You, C., H. Okano, S. Hui, Z. Zhang, M. Kim, C. Gunderson, Y. Wang, P. Lenz, D. Yan, and T. Hwa. 2013. Coordination of bacterial proteome with metabolism by cyclic AMP signalling. Nature. 500: 301–6.

32. Raue, A., M. Schilling, J. Bachmann, A. Matteson, M. Schelker, M. Schelke, D. Kaschek, S. Hug, C. Kreutz, B.D. Harms, F.J. Theis, U. Klingmüller, and J. Timmer. 2013. Lessons learned from quantitative dynamical modeling in systems biology. PLoS One. 8: e74335.

33. Dhooge, A., W. Govaerts, and Y. Kuznetsov. 2003. MATCONT: A MATLB package for numerical bifurcation analysis of ODEs. ACM T Math Softw. 29: 141–164.

34. Narang, A. 2007. Effect of DNA looping on the induction kinetics of the lac operon. J. Theor. Biol. 247: 695–712.

35. Studdert, C.A., and J.S. Parkinson. 2005. Insights into the organization and dynamics of bacterial chemoreceptor clusters through in vivo crosslinking studies. Proc. Natl. Acad. Sci. U. S. A. 102: 15623–8.

36. Kremling, A., K. Bettenbrock, B. Laube, K. Jahreis, J.W. Lengeler, and E.D. Gilles. 2001. The organization of metabolic reaction networks. III. Application for diauxic growth on glucose and lactose. Metab. Eng. 3: 362–79.

37. Bjarnason, J., C.M. Southward, and M.G. Surette. 2003. Genomic profiling of iron-responsive genes in Salmonella enterica serovar typhimurium by high-throughput screening of a random promoter library. J. Bacteriol. 185: 4973–82.

38. Tanaka, S., S.A. Lerner, and E.C. Lin. 1967. Replacement of a phosphoenolpyruvate-dependent phosphotransferase by a nicotinamide adenine dinucleotide-linked dehydrogenase for the utilization of mannitol. J. Bacteriol. 93: 642–8.

39. Miller, J.H. 1992. A Short Course in Bacterial Genetics. New York: Cold Spring Harbor Laboratory Press.

40. Booth IR, Mitchell WJ, H.W. 1979. Quantitative analysis of proton-linked transport systems. The lactose permease of Escherichia coli. Biochem J. 182: 687–696.

41. Klumpp, S., Z. Zhang, and T. Hwa. 2009. Growth Rate-Dependent Global Effects on Gene Expression in Bacteria. Cell. 139: 1366–1375.

42. Afroz, T., K. Biliouris, Y. Kaznessis, and C.L. Beisel. 2014. Bacterial sugar utilization gives rise to distinct single-cell behaviours. Mol. Microbiol. 93: 1093–103.

43. Bhogale, P.M., R.A. Sorg, J.-W. Veening, and J. Berg. 2015. What makes the lac-pathway switch: identifying the fluctuations that trigger phenotype switching in gene regulatory systems. Nucleic Acids Res. 42: 11321–8.

44. Choi, P.J., L. Cai, K. Frieda, and X.S. Xie. 2008. A stochastic single-molecule event triggers phenotype switching of a bacterial cell. Science. 322: 442–6.

45. Scott, M., T. Hwa, and B. Ingalls. 2007. Deterministic characterization of stochastic genetic circuits. Proc. Natl. Acad. Sci. 104: 7402–7.

46. Weber, M., and J. Buceta. 2013. Stochastic stabilization of phenotypic States: the genetic bistable switch as a case study. PLoS One. 8: e73487.

47. Kuhlman, T.E., and E.C. Cox. 2012. Gene location and DNA density determine transcription factor distributions in Escherichia coli. Mol. Syst. Biol. 8: 111–118.

48. Cohn, M., and K. Horibata. 1959. Inhibition by glucose of the induced synthesis of the beta-galactoside-enzyme system of Escherichia coli. Analysis of maintenance. J. Bacteriol. 78: 601–12.

49. Thattai, M., and A. van Oudenaarden. 2004. Stochastic gene expression in fluctuating environments. Genetics. 167: 523–30.

50. Nuoffer, C., B. Zanolari, and B. Erni. 1988. Glucose permease of Escherichia coli. The effect of cysteine to serine mutations on the function, stability, and regulation of transport and phosphorylation. J. Biol. Chem. 263: 6647–55.

51. Bettenbrock, K., S. Fischer, A. Kremling, K. Jahreis, T. Sauter, and E.-D. Gilles. 2006. A quantitative approach to catabolite repression in Escherichia coli. J. Biol. Chem. 281: 2578–84.